Journal of Nuclear Materials 393 (2009) 513–517

Contents lists available at ScienceDirect

Journal of Nuclear Materials

journal homepage: www.elsevier.com/locate/jnucmat

Generation of **c**-component edge dislocations in α-zirconium during neutron irradiation – An atomistic study

C.H. Woo *, Xiangli Liu [1]

Department of Electronic and Information Engineering, The Hong Kong Polytechnic University, Hung Hom, Kowloon, Hong Kong SAR, China

ARTICLE INFO

Article history:
Received 15 April 2009
Accepted 27 July 2009

ABSTRACT

The nucleation and multiplication of **c**-component edge dislocation segments during neutron irradiation in zirconium and its alloys is known to have important consequences to their in-reactor deformation behavior. Although there are ample experimental observations showing the close correlation between the edge-type and the screw-type of **c**-dislocations, the relation between them is unclear. In this paper, we performed atomistic study of the interaction between a [0 0 0 1] screw dislocation and a vacancy cluster in the form of a platelet on the basal plane. The local minimum-energy configuration was obtained using the conjugate-gradient method, with boundary relaxation achieved via a modified Green's function method. Under stress-free conditions, the vacancy clusters maintained their cavity nature. With a [0 0 0 1] screw dislocation in the close neighborhood, vacancy clusters containing more than 23 vacancies collapse into faulted vacancy loops. Interaction at even closer range leads to the disappearance of the vacancy cluster and the development of an edge component on the originally straight screw dislocation in the form of a helical line. The implications of these findings are discussed in relation to the experimentally observed behavior of growth acceleration in zirconium and its alloys.

1. Introduction

The change of the core structure of dislocations when interacting among themselves, or with various other crystal defects, is known to play an important role in the dimension stability and mechanical properties of the crystal. This is particularly true under irradiation-damage conditions. Atomistic simulations of interactions between edge dislocations and defect clusters, such as voids, SFTs (stacking fault tetrahedra) and SIA (self-interstitial atom) clusters have been performed for such studies in bcc and fcc metals [1–6].

Crystallographic anisotropy of important nuclear materials that do not have cubic crystal structure, such as graphite, uranium, zirconium and its alloys, introduces additional complexity into their microstructure evolution and concomitant materials property changes due to irradiation damage. For example, exposure of these metals to a fast neutron flux produces a shear deformation even absent an applied stress, a phenomenon known as irradiation growth [7,8]. The growth strain is the result of segregation of vacancies and interstitials, not unlike void swelling in the cubic metals, except that the associated dimensional changes are volume conserved in the form of pure shears. This phenomenon has been investigated in detail in hexagonal-close-pack (hcp) α-zirconium and its alloys [7–11], important structural materials for fission reactors.

It is well known [7–10] that models based on the assumption of a stable steady-state microstructure yield growth strain that increases linearly with the neutron dose. On the other hand, in a wide range of metallurgical states ranging from annealed or recrystallized Zircaloy to cold-worked Zircaloy-2 or -4, zirconium alloys show a super-linear growth behavior up to very high doses. In all cases, the onset of growth acceleration has been found to correlate with the increase of the line densities of **c**-component dislocations, through the multiplication of either line segments of edge character or the nucleation and growth of faulted vacancy loops lying on basal planes [8,10].

Although the relationship between growth acceleration and the increase of **c**-component dislocations with edge character can be well explained within the DAD theory of irradiation growth [9,10], yet the circumstances under which the edge-components emerge and continues to increase with irradiation dose remain hazy. A distinct possibility is that they might have come from the collapse of vacancy clusters that are known to play a primary role in the microstructure development and the associated macroscopic property changes of nuclear materials. However, electron irradiation of zirconium thin foils in HVEM at 573 K suggested that void nuclei in Zr took the form of thin plates

* Corresponding author. Tel.: +852 2766 6646.
E-mail address: Chung.woo@polyu.edu.hk (C.H. Woo).
[1] Present address: Harbin Institute of Technology at the Shenzhen Graduate School, Shenzhen, China.

0022-3115/$ - see front matter © 2009 Elsevier B.V. All rights reserved.
doi:10.1016/j.jnucmat.2009.07.013

on the basal planes [7,11,12], indicating that vacancy clusters in Zr in this form is stable and does not collapse spontaneously. The observation that the density of these loops is correlated with the grain orientation suggests that their nucleation could be related to the stress field experienced by the vacancy clusters [10]. Even if this is the case, the mechanistic origin of the correlation and how the screw dislocations are involved [7–11] still seek an explanation. In this paper, we study directly the reaction between a screw dislocation having the Burgers vector $\mathbf{b} = [0\,0\,0\,1]$ and a vacancy cluster in the form of thin plates on the basal plane, using an atomistic model. We will investigate the stability of vacancy clusters and study the possibility of core structure change of the screw dislocation as a result of the interaction. To overcome the relatively slow reaction kinetics of the process, a static, instead of dynamic, approach is followed. The paper is organized as follows. Section 2 describes the method and the computational details. The calculated results are presented and analyzed in Section 3, a short summary is given in Section 4.

2. Methodology and computational details

2.1. Inter-atomic potential and initial configurations

We use a Finnis–Sinclair-type many-body inter-atomic potential derived by Ackland for α-zirconium [13], in which the total energy E can be written as:

$$E = \sum_{i}^{N}\left[\sum_{j>i}^{N} V(x_{i,j}) - \rho_i^{\frac{1}{2}}\right], \tag{1}$$

where

$$\rho_i = \sum_{j=1}^{N} \phi(x_{ij}). \tag{2}$$

In Eq. (1), V and ϕ are pairwise functions between atoms i and j separated by a distance of x_{ij}. This potential has been tested in the calculation of lattice constants, formation energies and configurations of point defects, displacement cascades during irradiation damage and phase transition [13–15].

We use a rectangular simulation box (Fig. 1) with sides of 13.72 nm, 13.58 nm and 13.54 nm, respectively along the $[1\,1\,\bar{2}\,0]$, $[1\,\bar{1}\,0\,0]$ and $[0\,0\,0\,1]$ directions, containing a total of about 60,000 atoms. Experiments on nucleation and growth of cavities in electron-irradiated thin films [7,11,12] suggest that vacancy clusters exist in zirconium as circular platelets on $(0\,0\,0\,1)$ planes. Accordingly, vacancy clusters are considered for four different sizes with respective radii of 0.52 nm (nine vacancies), 0.78 nm (23 vacancies), 1.15 nm (45 vacancies) and 1.56 nm (85 vacancies). The unrelaxed $[0\,0\,0\,1]$ screw dislocation is introduced according to linear-elasticity theory at the center of the simulation box [16]. The equilibrium (i.e., force-free) configurations are then obtained using the standard conjugate-gradient method with flexible boundaries [17,18] as the local energy minimum.

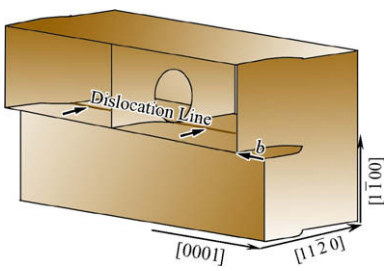

Fig. 1. Simulation cell containing the screw dislocation and vacancy cluster platelet. The vacancy cluster platelet in its habit plane is denoted by the solid circle and the core of the screw dislocation with Burgers vector $[0\,0\,0\,1]$ is denoted by the solid line in the center.

2.2. Flexible boundaries

Flexible boundaries are designed to eliminate, using a Green's function, residual forces on atoms in the boundary region due to atomic displacements in the core region. In our earlier work [17], the elastic Green's function was used for large distances between the source point and the field point, and the lattice Green function is used for shorter distances. This combination of the elastic and lattice Green's function has been widely regarded as the most effective flexible boundary scheme for two-dimensional simulations. To consider three dimensional (3D) problems, Rao et al. [18] developed a method using the Green function for point forces instead of line forces. However, efficiency and accuracy issues present some major drawbacks of the 3D flexible boundary method. To overcome such problems, we have used a modified relaxation procedure in [19] to study the Paidar–Pope–Vitek lock formation in Ni_3Al, in which the positions of only a fraction of the boundary atoms are updated and the procedure is iterated to convergence. To implement the flexible boundary method, the simulation cell is divided into three regions, namely, an atomistic region (region I), in which the atoms are located in the innermost part of the simulation cell, a Green's boundary region (region II), which is the boundary region of region I, in which the atomic positions are updated during the relaxation by the lattice and elastic Green's functions, and an outermost region III, which is required for the calculation of the Green's functions in region II. Usually, region II and region III together is regarded as the boundary region. In the work reported in this paper, region I has dimensions 11.44 nm × 11.30 nm × 11.26 nm along the $[1\,1\,\bar{2}\,0]$, $[1\,\bar{1}\,0\,0]$ and $[0\,0\,0\,1]$ directions, respectively. Regions II and III have thicknesses of 0.57 nm, which is also the cut-off radius of the potential. Following [19], displacements of the boundary atoms are set to a fraction, say 20%, of the value calculated by the Green's function.

In this simulation, the boundary region is updated once every 20 steps to eliminate the boundary forces. In between successive boundary updates, forces accumulate as region I relaxes. However, with an appropriate frequency of boundary updates and a partial use of the Green's functions, relaxation of the forces in both regions can be very efficiently performed (see Fig. 2).

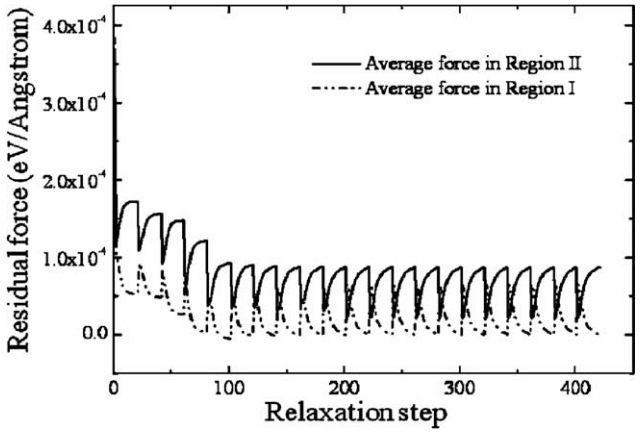

Fig. 2. Average residual forces in region I (atomistic region) and region II (boundary region) vs. relaxation steps during typical simulation of interaction between the screw dislocation and vacancy cluster platelet.

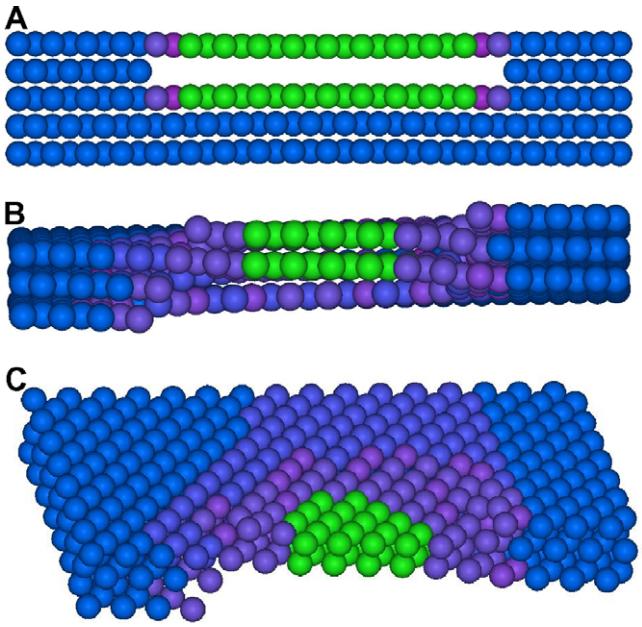

Fig. 3. Relaxed configuration of the vacancy cluster platelet (85 vacancies). (A) In the absence of the screw dislocation, and (B) in the presence of the screw dislocation. The vacancy cluster platelet is stable in the absence of the screw dislocation. In the presence of the screw dislocation, it collapses into a staking-fault. C is the top view of B. The colors of atoms describe the magnitude of their slip vectors (see text).

3. Results

To visualize the configuration of the lattice defect, we define in analogy with the Burgers vector of a dislocation a slip vector $\mathbf{s}^{\mu}$ for each atom μ:

$$\mathbf{s}^{\mu} = -\frac{1}{n_s}\sum_{\mu \neq \nu}(\mathbf{x}^{\mu\nu} - \mathbf{X}^{\mu\nu}), \tag{3}$$

where $\mathbf{x}^{\mu\nu}$ is the vector connecting the atom μ with its nearest neighbor ν in the current lattice, and $\mathbf{X}^{\mu\nu}$ is similarly defined for atoms in the reference lattice, i.e., the perfect crystal, in this case. n_s is the number of neighbors considered.

Fig. 3 shows the change in the atomistic configuration of an 85-vacancy cluster platelet on the basal plane, as it is brought near a **c**-Burgers vector screw dislocation. Atoms colored green[2] have the largest slip vectors and experience the largest lattice distortion around them, while those colored blue have the smallest slip vector with the smallest lattice distortion. Fig. 3A shows the relaxed vacancy cluster far away from the screw dislocation. The vacant lattice sites are clearly visible. We note that the uncollapsed configuration of the vacancy cluster is consistent with the structure of small cavities in zirconium thin films found at low dose during electron irradiation [7,11,12]. When the vacancy cluster is brought into the strain field near the screw dislocation, it collapses into a faulted loop lying on the basal plane with a **c**-component Burgers vector, as shown in Fig. 3B and Fig. 3C (top view of B configuration).

Fig. 4 is the relaxed configuration of the interacting region of an 85-vacancy cluster and the screw dislocation. A helical dislocation line that combines the edge character of the loop and the screw character of the impinging dislocation enclosing a faulted region is clearly visible. Here, atoms with slip vectors between 1.2 and 2.5 Å are identified and colored to visualize the defect configuration. Studies involving clusters of 45 and 23 vacancies have also been performed and the results shown in Fig. 5 and Fig. 6, respectively. The development of a similar edge component enclosing a stacking fault from the interacting **c**-type screw dislocation can also be seen.

[2] For interpretation of color in Figs. 3, 4, 7, the reader is referred to the web version of this article.

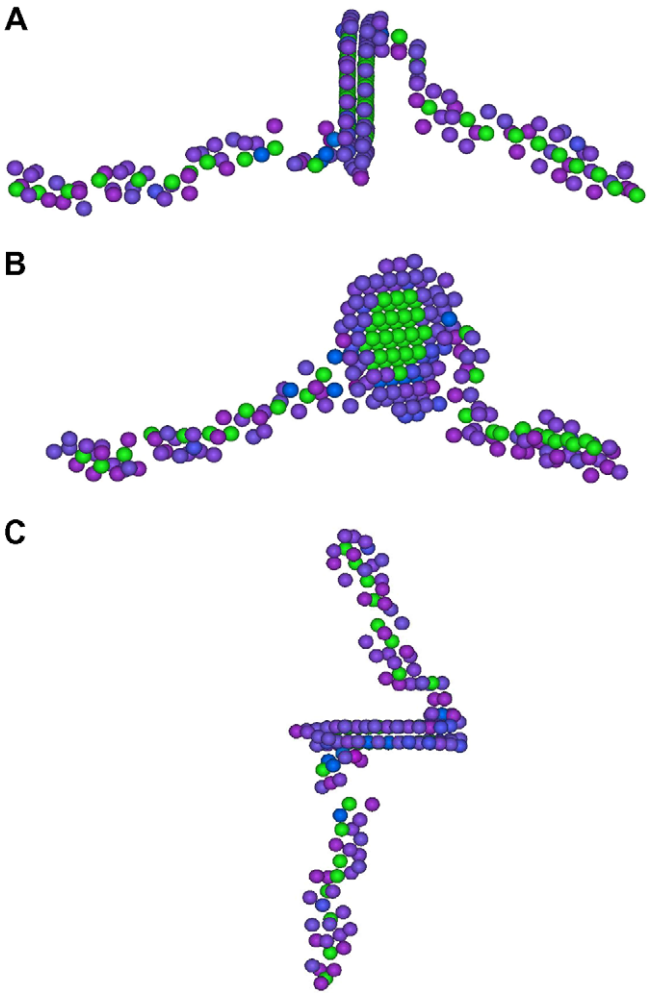

Fig. 4. (A) horizontal side view, (B) side view with the dislocation line partly in the plane of the paper, and (C) vertical side view of the relaxed configuration of vacancy cluster platelet (85 vacancies) in the presence of the screw dislocation, the dislocation line becomes helical and a staking-fault is generated in the original habit plane of the vacancy cluster. The colors of atoms describe the magnitude of their slip vectors.

Fig. 7 shows a different result for the 9-vacancy cluster with a radius of 0.52 nm, which is completely annihilated without collapsing and the trace of a faulted region. The relaxed configuration shows that the original straight dislocation line develops a component perpendicular to the **c**-direction. This may be interpreted as due to the absorption of vacancies into the screw dislocation.

4. Discussions

Irradiation-damage accumulation begins with intra-cascade clustering which plays a primary role in the development of irradiation-induced microstructure because of their dual function as both sources and sinks of point defects [20]. Most MD simulation work on displacement cascades in the hcps show that cascade morphology depends on crystal structure. In the case of hcp Zr, both vacancy and interstitial clusters are found in the cascade region after annealing, taking the form of **a**-loops, i.e., perfect pris-

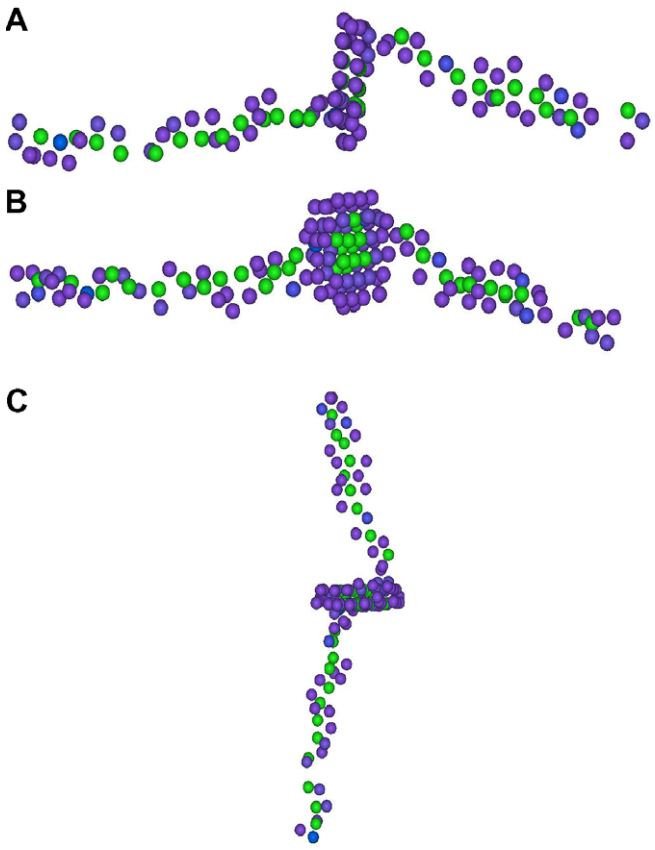

Fig. 5. Same as Fig. 4 for a vacancy cluster platelet of 45 vacancies.

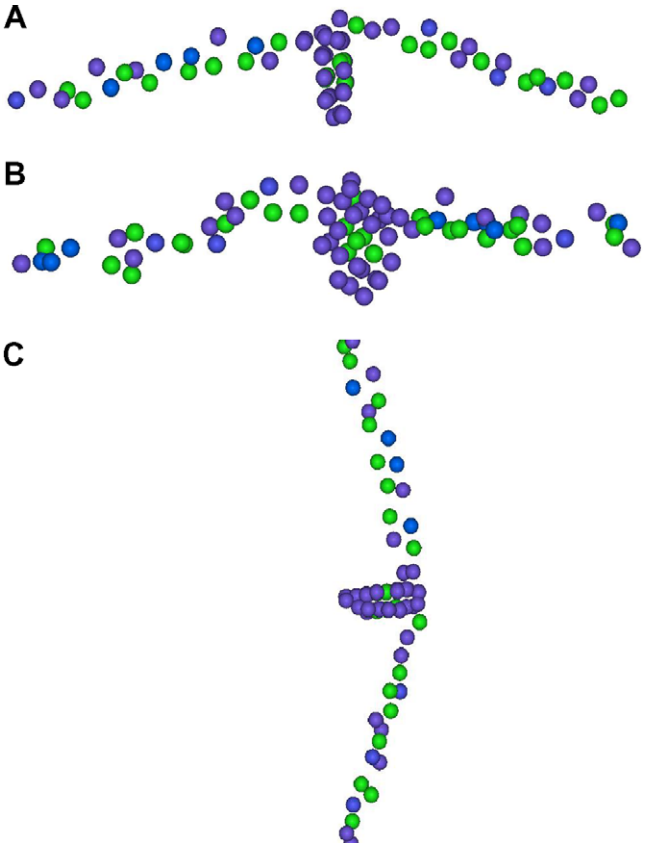

Fig. 6. Same as Fig. 4 for a vacancy cluster platelet of 23 vacancies.

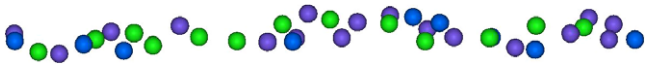

Fig. 7. Relaxed configuration of the smallest vacancy cluster platelet (nine vacancies) in the presence of the screw dislocation, the dislocation line keeps straight and no staking-fault is generated. The colors of the atoms describe the magnitude of their slip vectors.

matic dislocation loops with Burgers vector $\frac{1}{3}\langle 11\bar{2}0\rangle$ [21–23]. Defect clusters in the form of basal loops are seldom seen. These results are consistent with observed irradiation damage in Zr, which is dominated by $\frac{1}{3}\langle 11\bar{2}0\rangle$ perfect prismatic dislocation loops (**a**-loops) of both vacancy and interstitial character [7,8,24,25].

Indeed, at or below 673 K the number densities of interstitial and vacancy loops are found to be almost equal. The vacancy loops are elliptical in shape and are arranged randomly within sheets parallel to the basal plane, and the interstitial loops which tend to be circular and exist between the sheets of vacancy loops. The coexistence of vacancy and interstitial loops in the observed morphology has been well established on the basis of diffusional anisotropy difference (DAD) [7–9], which has been directly verified via atomistic simulation [26]. We note that this behavior is unlike the cubic metals where dislocation loops are primarily interstitial in nature.

Above 723 K the population of vacancy **a**-loops abruptly drops to below 20%. This reduction of the vacancy loops is consistent with the dissolution of the intra-cascade vacancy clusters at temperatures above annealing stage V, as predicted by the production bias theory [20]. In this temperature range, the vacancy clusters have a short mean lifetime, and most of them thermally dissociate into free vacancies almost immediately after formation. This results in a strongly reduced probability of nucleation of vacancy **a**-loops. The interstitial clusters, on the other hand, remain intact. The supersaturation of vacancies, as a result, becomes well above that of interstitials, producing the classical condition under which production bias becomes the dominant driving force for microstructure evolution [20]. In this connection, our present simulation results (Fig. 3) confirm the feasibility that small cavities condensed from supersaturated vacancies in Zr may exist as a faceted, uncollapsed void platelet on the basal plane under stress-free conditions.

Experimentally, electron irradiation of Zr at 573 K at a dose rate of $\sim 10^{-2}$ dpa/s in a HVEM [27] shows that cavities nucleate as thin plates on the basal plane, and then undergo morphology change with further irradiation, shortening along the **a**-directions and thickening along the **c**-direction. Cavity nucleation in the form of thin plates on the basal plane has also been reported in electron-irradiated Zr samples pre-irradiated in DFR at 740 K [11].

Irradiation growth in zirconium is well known to be sensitive to the microstructure development during irradiation [8,28,29]. For annealed Zircaloy, the pre-irradiation microstructure contains grain boundaries ($\sim$10 μm grain size) and a very low network dislocation density ($\sim 10^{13}/m^2$). A high density of both **a**-type vacancy and interstitial dislocation loops (with normals in the basal plane) in the early stage of irradiation. The fraction of **a**-type vacancy loops increases steadily with temperature in the low and medium temperature regimes, but drops abruptly in the high-temperature regime [24,25]. The steady irradiation growth rate in this temperature range is relatively low ($<10^{-4}$/NRT dpa in the longitudinal direction) [28,29]. In the medium and high-temperature regimes, large faulted basal **c**-component vacancy loops appears after a critical neutron dose, corroborated very well with a strongly increased growth rate [30,31]. Indeed, in the high-temperature regime, the growth behaviors of annealed and cold-worked materials become nearly indistinguishable [32]. This large increase in growth rates

at high temperatures bears a lot of resemblance to the behavior of the swelling rates in cubic metals under the operation of production bias [20].

In cold-worked zirconium alloys, a network of **a** and c + **a** dislocations dominate the pre-irradiation dislocation structure [33,34]. Similar to annealed materials, an **a**-loop structure also develops in the early stage of irradiation. The growth rate increases with the cold work, and are relatively high at all temperature regimes and all fast neutron dose [8,28,29]. The formation of faulted loops on the basal planes from **c**-component dislocations undergoing helical climb has also been reported. It is well known that increasing the density of **c**-component dislocations invariably accelerates the growth rate [35].

Edge-component dislocations with **c**-type Burgers vectors can also evolve from faulted basal loops of edge character with Burgers vector $\frac{1}{6}\langle 20\bar{2}3\rangle$, which are commonly found in irradiated Zr samples in the temperature range between 560 and 773 K. Experimental observations [7,8,11,33–35] of faulted vacancy loops on the basal plane growing to sizes up to 0.1–1 μm in diameter are common. These loops are invariably vacancy in nature and are very often found with **c**-type screw dislocations threading through them [8,10–12,33–35]. According to the present simulation results, their presence may be explained by the interaction between a vacancy platelet and a **c**-component screw dislocation.

The generation of loops of this kind has very important consequences on the further evolution of the microstructure and the associated macroscopic deformation. Diffusion anisotropies of the vacancies and interstitials calculated [26] with Ackland's many-body inter-atomic potential [13] shows that the dislocation segments of these loops have a large DAD bias towards vacancies [9]. As irradiation proceeds, the net vacancy flow into these loops progressively adds new line segments to this class of dislocations. Holt et al. [10] showed that starting from a metallurgical state with a low density ρ_c of **c**-component edge-dislocation line segments, an increase of the ratio ρ_c/ρ_a increases the segregation of vacancies and the interstitials to the basal and prismatic crystallographic planes leading to an enhancement of the growth rate. Here ρ_a is the density of the **a**-type dislocations of edge character. We note that these results are based only on the crystal symmetry and the inter-atomic potential, and are in very good agreement with a large amount of observations in experimental work [7–12] despite their non-empirical nature.

5. Summary and conclusions

The interactions between screw dislocations and various sizes of vacancy cluster platelets are simulated using the standard conjugate-gradient method and modified flexible Green's function boundary condition. The results show that in the absence of the screw dislocation, the vacancy cluster is stable in form of platelet in (0 0 0 1) planes, consistent with experimental observations of the presence of cavity platelets in Zr. For sufficiently large vacancy clusters, the interaction with a **c**-type screw dislocation causes their collapse into a faulted loop on the basal plane threaded by the dislocation. There is a critical size (~9 vacancies) under which the collapse of vacancy clusters into faulted loop does not occur. The interaction between the large vacancy cluster platelet and the screw dislocation produces a change of the core structure resulting in the straight dislocation line becoming helical, enclosing a stacking fault. At the same time, the pure screw dislocation generates an edge component located in the previous habit plane of the vacancy cluster platelet. As pointed out in the foregoing, the generation of the staking-fault is very important to the further evolution of microstructure. Under irradiation, the faulted vacancy loops cannot move by glide, but will continuously expand in the basal plane until it meets the existing microstructure. Un-faulted clusters will expand into a cavity due to the DAD of the interstitials and vacancies in hcp metals.

Acknowledgements

The authors are grateful for funding support by research grants PolyU5305/07E PolyU5320/08E.

References

[1] D. Rodney, G. Martin, Phys. Rev. B 61 (2000) 8714.
[2] D. Rodney, G. Martin, Phys. Rev. Lett. 82 (1999) 3272.
[3] J.O. Stiegler, E.E. Bloom, Radiat. Eff. 8 (1971) 33.
[4] M. Kiritani, J. Nucl. Mater. 216 (1994) 220.
[5] Yu.N. Osetsky, D.J. Bacon, B.N. Singh, B. Wirth, J. Nucl. Mater. 307 (2002) 852.
[6] X. Liu, S.I. Golubov, C.H. Woo, H. Huang, Comp. Mod. Eng. Sci. 5 (2004) 527.
[7] C.H. Woo, J. Nucl. Mater. 276 (2000) 90.
[8] R.A. Holt, J. Nucl. Mater. 372 (2008) 182.
[9] C.H. Woo, J. Nucl. Mater. 159 (1988) 237.
[10] R.A. Holt, A.R. Causey, N. Christodoulou, M. Griffith, E.T.C. Ho, C.H. Woo, ASTM STP 1295 (1996) 623.
[11] C.H. Woo, R.A. Holt, M. Griffiths, Materials Modeling: From Theory to Technology, Institute of Physics Publishing, Bristol and Philadelphia, 1992. pp. 55–60.
[12] M. Griffiths, D. Gilbon, C. Regnard, C. Lemaignan, J. Nucl. Mater. 205 (1993) 237.
[13] G.J. Ackland, S.J. Wooding, D.J. Bacon, Philos. Mag. A 71 (1995) 553.
[14] S.J. Wooding, D.J. Bacon, Philos. Mag. 76 (1997) 1033.
[15] O.F. Sankey, D.J. Niklewsky, D.A. Drabold, J.D. Dow, Phys. Rev. B 41 (1990) 12750.
[16] A.N. Stroh, Philos. Mag. 3 (1958) 625.
[17] C.H. Woo, M.P. Puls, Philos. Mag. 25 (1977) 727.
[18] S. Rao, C. Hernandez, J.P. Simmons, T.A. Parthasarathy, C. Woodward, Philos. Mag. A 77 (1998) 231.
[19] A.H.W. Ngan, M. Wen, C.H. Woo, Comput. Mater. Sci. 29 (2004) 259.
[20] C.H. Woo, B.N. Singh, Philos. Mag. A 65 (1992) 889.
[21] S.J. Wooding, D.J. Bacon, Philos. Mag. A76 (1997) 1033.
[22] A.G. Mikhin, N. De Diego, D.J. Bacon, Philos. Mag. A75 (1997) 1153.
[23] D. Bacon, J. Nucl. Mater. 251 (1988) 176.
[24] A. Jostsons, P.M. Kelly, R.G. Blake, K. Farrell, ASTM STP 683 (1979) 46.
[25] A. Jostsons, P.M. Kelly, R.G. Blake, J. Nucl. Mater. 66 (1977) 236.
[26] C.H. Woo, X. Liu, Philos. Mag. 87 (2007) 2355.
[27] M. Griffiths, R.W. Gilbert, C.E. Coleman, J. Nucl. Mater. 159 (1988) 405.
[28] R.G. Fleck, R.A. Holt, V. Perovic, J. Tadross, J. Nucl. Mater. 159 (1988) 75.
[29] A. Rogerson, J. Nucl. Mater. 159 (1988) 43.
[30] R.A. Holt, R.W. Gilbert, J. Nucl. Mater. 137 (1986) 185.
[31] R.A. Holt, J. Nucl. Mater. 159 (1988) 310.
[32] R.P. Tucker, V. Fidleris, R.B. Adamson, ASTM STP 804 (1984) 427.
[33] M. Griffiths, J. Nucl. Mater. 159 (1988) 190.
[34] M. Griffiths, J. Nucl. Mater. 205 (1993) 205.
[35] M. Griffiths, R.A. Holt, A. Rogerson, J. Nucl. Mater. 225 (1995) 245.